

η^1 -P_{basal} Coordination of P₄X₃ (X = S, Se) Molecules toward 16e Ruthenium Fragments

Massimo Di Vaira,^[a] Isaac de los Rios,^[a] Fabrizio Mani,^[a] Maurizio Peruzzini,^[b] and Piero Stoppioni*^[a]

Keywords: Ruthenium / Cyclopentadienyl ligands / Bidentate ligands / Density functional calculations

Ruthenium(II) pentamethylcyclopentadienyl complexes [Ru(η^5 -C₅Me₅)Cl(L-L)] [L-L = 1,2-bis(diphenylphosphanyl)ethane, dppe (1), bis(diphenylphosphanyl)methane, dppm, *cis*-1,2-bis(diphenylphosphanyl)ethylene, dppet, and (1-diphenylarsanyl-2-diphenylphosphanyl)ethane, dpadppe] treated with a stoichiometric amount of P₄X₃ (X = S, Se) in THF have yielded the compounds [Ru(η^5 -C₅Me₅)(L-L)-(P₄X₃)]BPh₄ (X = S, Se). In the P₄Se₃ derivatives the heptatomic cage is bound to the metal through a basal phosphorus atom. The P₄S₃ derivatives have been obtained as pairs of coordination isomers, with the cage linked either through the apical or through one of the basal P atoms, the latter form

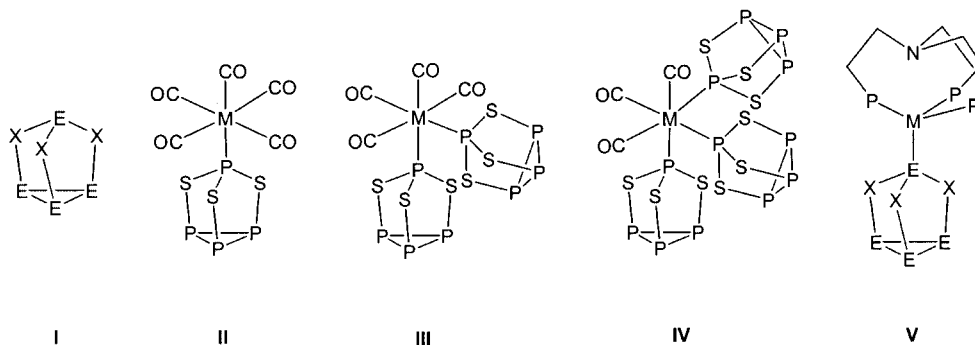
predominating (95% abundance), irrespective of the L-L ligand. The monometal complex [Ru(η^5 -C₅Me₅)(dppe)(η^1 -P_{basal}-P₄Se₃)]BPh₄ reacts with 1 to afford the dimetal compound [(Ru(η^5 -C₅Me₅)(dppe))₂(μ , $\eta^{1:1}$ -P_{basal}-P_{apical}-P₄Se₃)]-(BPh₄)₂, where the cage exhibits both modes of bonding. The compounds have been characterized by NMR spectra (¹H, ¹³C and ³¹P) and elemental analyses. A theoretical analysis of the bonding properties of the two coordination isomer types is also presented.

(© Wiley-VCH Verlag GmbH & Co. KGaA, 69451 Weinheim, Germany, 2004)

Introduction

The mixed cage molecules E₄X₃ (E = P, As; X = S, Se) (Scheme 1, I) possess a unique structure exhibiting a pseudo-tetrahedral array of pnictogen atoms, where a homocyclic E₃ unit is connected via three bridging chalcogen atoms to a single pnictogen in the apical position.^[1] Their

behaviour towards transition metal fragments has been widely studied and various compounds containing E_mX_n units, which originate from the disruptive fragmentation of the heptatomic cages, particularly P₄S₃ and As₄S₃, have been described.^[2–6] Although such units, stabilized by the metal moieties, are considered to form through stepwise disruption and/or formation of E–E bonds following the in-



Scheme 1

^[a] Dipartimento di Chimica, Università di Firenze, via della Lastruccia n. 3, 50019 Sesto Fiorentino, Firenze, Italy

^[b] ICCOM-CNR, via Madonna del Piano, 50019 Sesto Fiorentino, Firenze, Italy
E-mail: piero.stoppioni@unifi.it

Supporting information for this article is available on the WWW under <http://www.eurjic.org> or from the author.

itial interaction of the intact E₄X₃ cage with the metal fragment, primary complexation of the cages has been accomplished only in few instances, e.g. with Lewis acidic metal fragments which, upon coordination, yield electronically saturated compounds having either octahedral, e.g. [M(CO)_{5-x}(η^1 -P₄S₃)_{1+x}] [Scheme 1: M = Mo, W; x = 0

(II);^[7] M = Cr, Mo, W; x = 1, (III);^[8] M = Cr, Mo; x = 2 (IV)^[8], or tetrahedral geometry in the presence of sterically protecting groups on the coligand, e.g. [(NP₃)M(η¹-P₄X₃)], V [NP₃ = tris(diphenylphosphanylethyl)amine; M = Ni,^[9] Pd;^[10] X = S, Se].

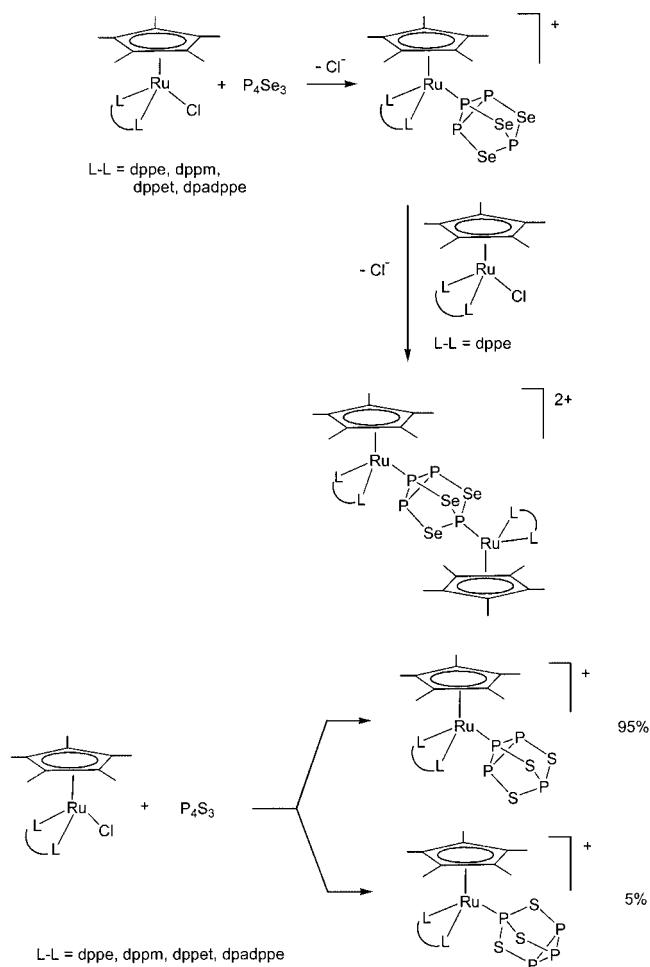
All of the above compounds, characterized by either X-ray diffraction analysis or ³¹P NMR spectroscopy, contain the cage bound to the metal through the apical phosphorus atom, which, accordingly, has been considered a better donor than a basal phosphorus atom. Recently the 16e [(triphos)Re(CO)₂]⁺ fragment^[11] [triphos = 1,1,1-tris(diphenylphosphanylmethyl)ethane] has yielded, in the presence of P₄X₃ (X = S, Se), a mixture of Re-η¹-P_{apical} and Re-η¹-P_{basal} complexes, the latter being predominant (ca. 87%). Both, apical and basal P₄X₃ complexes with the Lewis acids BBr₃, BI₃ and NbCl₅ have been reported.^[12] Conversely, P₄X₃ weak complexes with the silver ion have been reported in which the intact cage interacts with the metal through one sulfur and both the apical and one basal P atoms.^[13]

We report here on the synthesis and characterization of the family of novel η¹-tetraphosphorus trichalcogenide complexes [Ru(η⁵-C₅Me₅)(L-L)(η¹-P₄X₃)]BPh₄ [L-L = 1,2-bis(diphenylphosphanyl)ethane, dppe, bis(diphenylphosphanyl)methane, dppm, *cis*-1,2-bis(diphenylphosphanyl)ethylene, dppet, and (1-diphenylarsanyl-2-diphenylphosphanyl)ethane, dpadppe; X = S, Se]. In the P₄Se₃ derivatives the intact cage is bound to the metal fragment through a basal P atom. The P₄S₃ compounds present a mixture of Ru-η¹-P_{apical} and Ru-η¹-P_{basal} coordination isomers. All compounds have been characterized by NMR measurements. L-L ligands with different electronic and geometric requirements do not affect the binding properties of the metal fragments, which are highly specific for a basal phosphorus atom of the cage. The monometal complex [Ru(η⁵-C₅Me₅)(dppe)(η¹-P_{basal}-P₄Se₃)]BPh₄ yields, in the presence of [Ru(η⁵-C₅Me₅)Cl(dppe)], the dinuclear compound [{Ru(η⁵-C₅Me₅)(dppe)}₂(P₄Se₃)](BPh₄)₂ which combines the Ru-η¹-P_{apical} and Ru-η¹-P_{basal} coordination modes. Repeated attempts to obtain the compounds in crystalline form, suitable for X-ray investigations, failed. Their structures and bonding were then investigated by computational methods.

Results and Discussion

The pseudo-octahedral complexes [Ru(η⁵-C₅Me₅)Cl(L-L)] [L-L = ddpe (1), dppm (2), dppet (3), dpadppe (4)], which easily dissociate the chloride in solution,^[14–16] react in THF with one equivalent of P₄X₃ (X = S, Se) to form a brick-red solution. Upon addition of NaBPh₄ and after workup the compounds [Ru(η⁵-C₅Me₅)(L-L)(η¹-P₄X₃)]BPh₄ are isolated as microcrystalline solids in fairly good yield. The solids are soluble in CH₂Cl₂, THF and (CH₃)₂CO; they are stable under an inert atmosphere and may be handled in air for a limited time. Elemental analysis of the products confirms the formation of 1:1 adducts be-

tween the [Ru(η⁵-C₅Me₅)(L-L)]⁺ synthon and the P₄X₃ molecule. The formation of the P₄X₃ derivatives is sketched in Scheme 2.



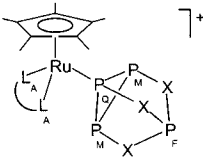
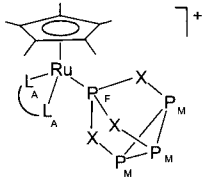
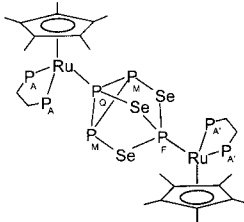
Scheme 2

The compounds have been characterized by ¹H, ¹³C{¹H} and ³¹P{¹H} NMR measurements. The intensity ratios of the ³¹P{¹H} signals accord with the proposed formulae; the NMR spectroscopic data of the uncoordinated and the coordinated P₄X₃ cages, and the labelling scheme used for the different phosphorus nuclei, are shown in Table 1.

Characterization of the P₄Se₃ Coordination Compounds

The P₄Se₃ derivatives [Ru(η⁵-C₅Me₅)(L-L)(P₄Se₃)]BPh₄ [L-L = dppe (5), dppm (6) and dppet (7)] exhibit in their ³¹P{¹H} NMR spectra an A₂FM₂Q spin system which is consistent with the P₄Se₃ cage molecule being bound to the metal through one basal phosphorus atom. The diposphane ligand P atoms (P_A) of each compound yield a doublet due to coupling with the P_Q atom of the cage bound to the metal; both the chemical shifts and coupling constants have values expected for ruthenium(II) half-sandwich compounds.^[10,14,17] The heptatomic cage yields the FM₂Q part of the spin system (Table 1). The two equivalent uncoordinated basal P_M atoms yield a doublet of doublets in the

Table 1. ³¹P{¹H} NMR spectroscopic data of the free and coordinated P₄Se₃ and P₄S₃ ligands

						
	5–8 (X = Se) 10–13 (X = S), major isomer		10–13 (X = S), minor isomer		9	
Compound	Chemical shift, δ (ppm) ^[a] P _F P _M /P _{M'} ^[b]		P _Q	Coupling constant, J (Hz) ² J (P _F –P _M) ² J (P _F –P _Q)		¹ J (P _M –P _Q)/ ¹ J (P _{M'} –P _Q) ^[b] ¹ J (P _M –P _{M'}) ^[b]
P ₄ Se ₃	30.7 (q)	–114.1 (d)		72.0		
5 ^[c]	68.4 (dt)	–125.4 (dd)	41.2 (dt)	59.5	51.0	244.0
6 ^[d]	67.7 (dt)	–131.2 (dd)	41.1 (dt)	60.5	52.0	243.8
7 ^[c]	59.3 (dt)	–125.3 (dd)	40.9 (dt)	64.1	49.8	244.1
8 ^{[d],[e]}	65.8 (dt)	–149.8 (dddd) –133.7 (ddd)	34.7 (dddd)	59.2	53.3	249.4 238.7 103.7
9 ^[c]	125.7 (dt)	–116.8 (dd)	20.6 (dt)	46.1	19.4	211.4
P ₄ S ₃	65.1 (q)	–127.3 (d)		70.0		
10 major isomer ^[c]	93.9 (dt)	–141.9 (dd)	35.5 (dt)	60.2	44.9	243.2
10 minor isomer	150.6 (m)	–120.5 (d)		22.8		
11 major isomer ^[c]	91.3 (dt)	–148.8 (dd)	29.7 (dt)	60.7	46.0	243.3
11 minor isomer	142.7 (m)	–114.9 (d)		15.0		
12 major isomer ^[c]	90.0 (dt)	–143.6 (dd)	31.9 (dt)	64.1	44.8	242.3
12 minor isomer	155.5 (m)	–119.4 (d)		20.4		
13 major isomer ^[c] ^[e]	90.4 (dt)	–149.8 (dddd) –143.4 (ddd)	34.7 (dddd)	61.5	47.0	244.8 236.4 101.8
13 minor isomer	147.2 (m)	–121.9 (d)		24.4		

^[a] NMR spectra were recorded at room temperature with a Varian Gemini g300bb spectrometer. Key: d = doublet, t = triplet, q = quadruplet, m = multiplet. ^[b] P_M atoms of compounds with the phosphars ligands **8** and **13** (major isomer) are diastereotopic. ^[c] Spectrum recorded in CD₂Cl₂. ^[d] Spectrum recorded in (CD₃)₂CO. ^[e] Only one P_A atom present.

spectra of **5**, **6** and **7**, characterized by a small coupling with P_F and a large one to P_Q (ca. 240 Hz). The dpadppe compound **8** exhibits an AFMM'Q spin system in which the two basal uncoordinated phosphorus atoms of the cage are diastereotopic for L–L ligands of different donors (one P and one As) which make the ruthenium atom chiral. The resonance of P_M atoms is moderately shielded with respect to the three equivalent basal P atoms of the free cage (Table 1), whereas the P_Q resonance is shifted notably downfield. The uncoordinated P_F apical atom of the cage in **5–8** yields a doublet of triplets which is slightly downfield shifted with respect to the free ligand. The spectra of compounds **5**, **6** and **7** do not change from –60 to +50 °C (³¹P NMR experiment in a sealed tube). Due to the limited solubility of the compounds ⁷⁷Se NMR spectra were not recorded.

The monometal compound [Ru(η⁵-C₅Me₅)(dppe)(P₄Se₃)]BPh₄ (**5**) dissolved in THF reacts with the chloride labile **1** to form, after workup, the dimetal species [{Ru(η⁵-C₅Me₅)(dppe)}₂(P₄Se₃)](BPh₄)₂ (**9**). The ³¹P NMR spectrum of the compound (Table 1) yields an A₂A'₂FM₂Q spin system, consistent with double metallation of the P₄Se₃ molecule, which holds the two non-equivalent [{Ru(η⁵-C₅Me₅)(dppe)] metal units together and is responsible for the FM₂Q part of the spin system. The coupling constants

of the two resolved multiplets due to the cage phosphorus atoms (the apical and a basal one) bound to the metal fragments are particularly useful to assign the signals of the dppe ligands in the two ruthenium fragments, occurring in a narrow region (71.1 and 72.0 ppm). The apical phosphorus atom of P₄Se₃ bound to the metal undergoes a significant downfield shift upon coordination; the same trend, although less pronounced, occurs for the [(triphos)Re(CO)₂(P₄Se₃)]⁺ cation.^[11] Although polymetallic cluster compounds containing two^[18] or three^[19] bridging P₄S₃ units, formed through activation of a P–P bond, and tetrametallic compounds containing the P₄Se₃ unit, resulting from the cleavage of P–P and P–Se bonds,^[6] have been described, the present dimetal species exhibits the intact P₄Se₃ molecule in a bridging position between two transition metal fragments, in analogy with the very recently reported P₄S₃ silver adducts.^[13]

Characterization of the P₄S₃ Coordination Compounds

The ³¹P{¹H} NMR spectra of the [Ru(η⁵-C₅Me₅)(L-L)(P₄S₃)]BPh₄ compounds [L–L = dppe (**10**), dppm (**11**), dppet (**12**) and dpadppe (**13**)] indicate a pair of coordination isomers, present in a ratio of ca. 19:1, that differ in the bonding mode of the P₄S₃ molecule to the metal fragment: either through the apical P or through one of the

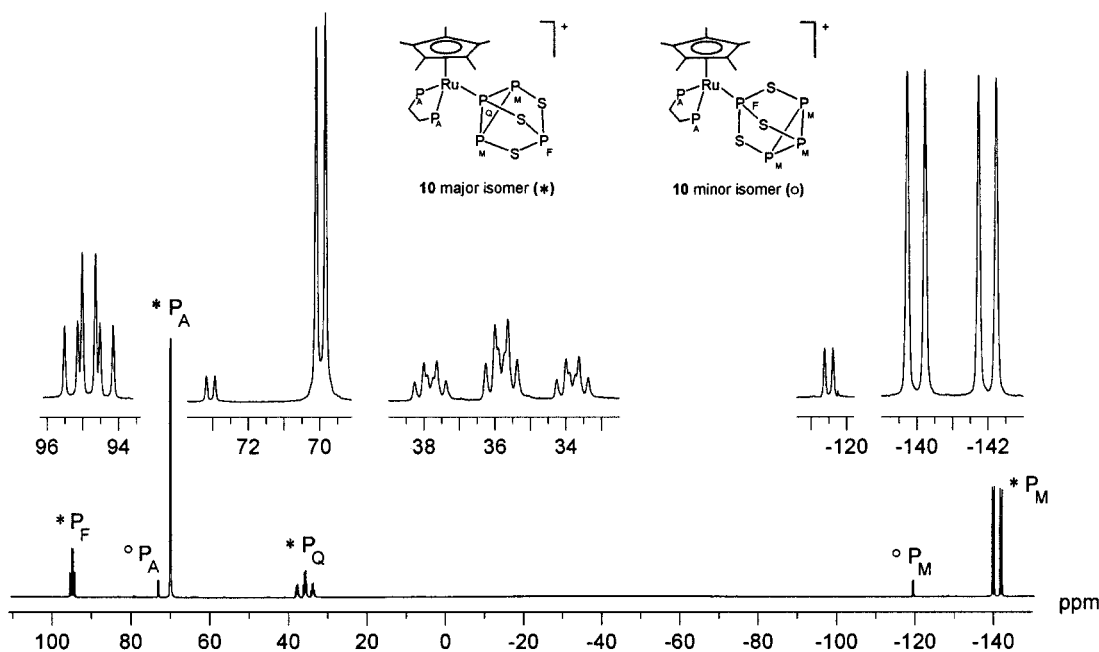


Figure 1. $^{31}\text{P}\{^1\text{H}\}$ NMR spectrum of $[\text{Ru}(\eta^5\text{-C}_5\text{Me}_5)(\text{dppe})(\text{P}_4\text{S}_3)]\text{BPh}_4$ in CD_2Cl_2 . The multiplet due to P_F of the minor isomer, a weak, broad signal at $\delta = 150.6$ ppm, is not reported.

basal P atoms (Scheme 2). This is supported by the $^{31}\text{P}, ^{31}\text{P}$ -2D COSY NMR spectra of **10** and **11**, which show two sets of correlated peaks. The $^{31}\text{P}\{^1\text{H}\}$ spectrum of $[\text{Ru}(\eta^5\text{-C}_5\text{Me}_5)(\text{dppe})(\text{P}_4\text{S}_3)]\text{BPh}_4$ (**10**) is shown in Figure 1.

The major isomers of **10**, **11** and **12** exhibit an $\text{A}_2\text{FM}_2\text{Q}$ spin system (Table 1), indicative of coordination by the cage through a basal P atom. The spectral features parallel those of the P_4Se_3 derivatives, with the cage accounting for the FM_2Q part of the spin system. The P_M signal is split, with unequal $\text{P}_\text{M}-\text{P}_\text{Q}$ and $\text{P}_\text{M}-\text{P}_\text{F}$ coupling constants, as found for **5**–**7** and the related rhenium compound $[(\text{triphos})\text{Re}(\text{CO})_2(\text{P}_4\text{S}_3)]^+$.^[11] The downfield shift of the P_Q signal is larger than that of the rhenium analog.^[11] As discussed above for **8**, the major isomer of the dpadppe derivative **13** exhibits an $\text{AFMM}'\text{Q}$ spin system due to the chirality of the metal atom. The chemical shifts and coupling constants are similar to those of the major isomers of **10**–**12**.

The minor isomers of **10**, **11** and **12** exhibit an A_2FM_3 spin system (Table 1), consistent with coordination of the intact cage to the metal via the apical P_F atom. The L–L ligand P_A atoms yield a doublet at the expected field. The FM_3 part of the splitting pattern, due to the cage, exhibits chemical shifts and coupling constants in agreement with those of the corresponding coordination isomer of the rhenium compound previously described.^[11] The signals of the P_4S_3 phosphorus atoms do not significantly depend on the ancillary L–L ligand (Table 1). Notably, the ruthenium-bonded P_F atom resonance occurs at low field (142–155 ppm) as a complex multiplet due to coupling with P_A and P_M ; the $\text{P}_\text{F}-\text{P}_\text{M}$ coupling constant is smaller than for the free cage (Table 1) and approaches that with the phosphane P_A . In keeping with the proposed structure,

the three basal P_M atoms afford a doublet due to coupling with P_F . The minor isomer of the dpadppe derivative, **13**, yields an AFM_3 spin system, as expected, due to the presence of only one magnetically active P atom in the dpadppe ligand. The $^{31}\text{P}\{^1\text{H}\}$ NMR spectra of **10**, **11** and **13**, obtained in the temperatures range -60 to $+50$ °C (experiment in a sealed tube), do not show any dynamic process and the relative amounts of the two isomers do not change. This rules out an equilibrium between the two species which, therefore, should form through independent interactions of the basal and the apical phosphorus atoms of the cage.

Quantum-Mechanical Calculations

In the absence of crystallographic structural data on the compounds quantum-mechanical calculations were undertaken to gain information on the geometries, the relative energies of isomers and to possibly rationalize structural preferences. As described in the Exp. Sect., building on results from preliminary calculations performed on models at various levels of accuracy, the geometry of the lowest-energy conformer found for each of the coordination modes of the cage molecule in the $[\text{Ru}(\eta^5\text{-C}_5\text{Me}_5)(\text{dppe})(\text{P}_4\text{S}_3)]^+$ cation (i.e., coordination through the apical phosphorus atom, P_apc hereafter, or through a basal one, P_bas), was optimized at the B3LYP/6–31G(d) level, with metal atom ECP functions.^[20] These two models will be referred to as **10apc** and **10bas**, respectively. After Se for S substitution in the former models and subsequent optimizations, models **5apc** and **5bas** for the $[\text{Ru}(\eta^5\text{-C}_5\text{Me}_5)(\text{dppe})(\text{P}_4\text{Se}_3)]^+$ cation were obtained. Representations of the **10apc** and **10bas** isomers are shown in Figure 2; those of the **5apc** and **5bas** models are similar and are given, with more details, with the Sup-

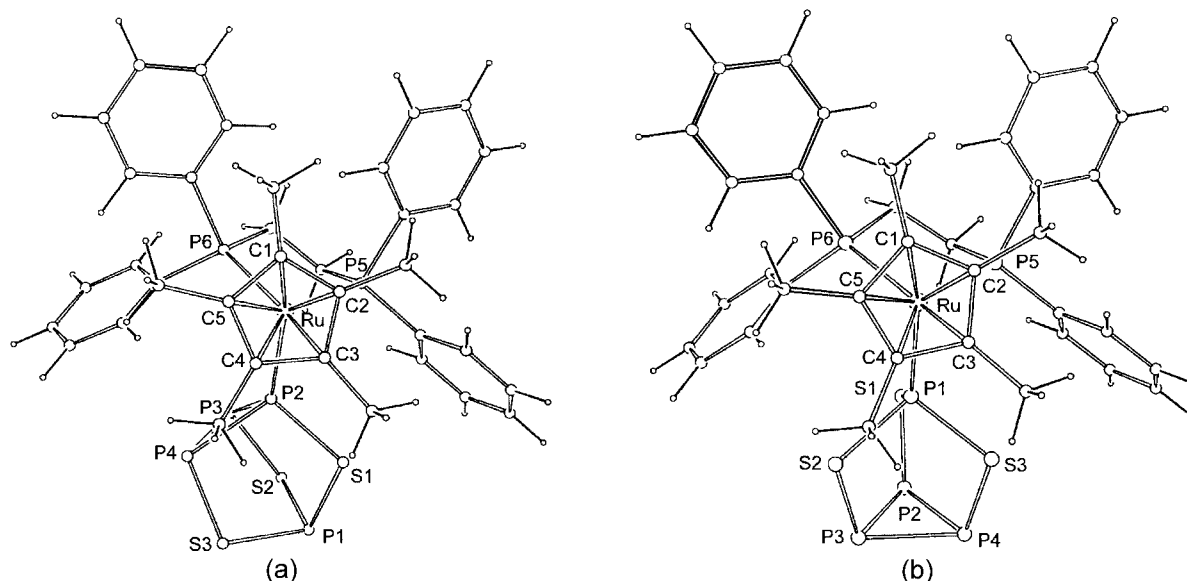


Figure 2. Optimized geometries for the $[\text{Ru}(\eta^5\text{-C}_5\text{Me}_5)(\text{dppe})(\text{P}_4\text{S}_3)]^+$ cation with the cage molecule coordinated (a) through a basal phosphorus atom, model **10bas**, and (b) through the apical phosphorus atom, model **10apc**.

Table 2. Relative energies ($\text{kJ}\cdot\text{mol}^{-1}$) and selected bond lengths (\AA) for the **10bas** and **10apc** models of $[\text{Ru}(\eta^5\text{-C}_5\text{Me}_5)(\text{dppe})(\text{P}_4\text{S}_3)]^+$ isomers and for the **5bas** and **5apc** models of $[\text{Ru}(\eta^5\text{-C}_5\text{Me}_5)(\text{dppe})(\text{P}_4\text{Se}_3)]^+$ isomers

	10bas ^[a]	10apc ^[a]	5bas ^[a]	5apc ^[a]
ΔE	0	9.11	0	13.39
Ru–P(5)	2.404	2.413	2.398	2.406
Ru–P(6)	2.425	2.448	2.428	2.445
Ru–C(1)	2.318	2.317	2.316	2.316
Ru–C(2)	2.342	2.345	2.339	2.343
Ru–C(3)	2.316	2.328	2.315	2.330
Ru–C(4)	2.324	2.358	2.329	2.367
Ru–C(5)	2.320	2.323	2.323	2.329
Ru–P(n) ^[b]	2.346	2.339	2.360	2.364
P(1)–S(1) ^[c]	2.129	2.173	2.266	2.323
P(1)–S(2)	2.165	2.175	2.305	2.326
P(1)–S(3)	2.164	2.163	2.303	2.309
S(1)–P(2)	2.151	2.122	2.300	2.262
S(2)–P(3)	2.126	2.118	2.266	2.257
S(3)–P(4)	2.124	2.120	2.264	2.260
P(2)–P(3)	2.285	2.287	2.282	2.280
P(2)–P(4)	2.284	2.289	2.278	2.281
P(3)–P(4)	2.293	2.289	2.283	2.280

^[a] Atomic labels as in Figure 2. ^[b] $n = 1$: **10apc** and **5apc**, $n = 2$: **10bas** and **5bas**. ^[c] Bond lengths (\AA) within the free cage molecules (possessing threefold symmetry), from calculations at the B3LYP/6–31G(d) level, are [averages of experimental values from ref.^[21] (P_4S_3) and refs.^[10,19,22] (P_4Se_3) in parentheses]: P_4S_3 , $\text{P}_{\text{apc}}\text{--S} = 2.150$ (2.06), $\text{P}_{\text{bas}}\text{--S} = 2.139$ (2.09), $\text{P}_{\text{bas}}\text{--P}_{\text{bas}} = 2.276$ (2.23); P_4Se_3 , $\text{P}_{\text{apc}}\text{--Se} = 2.276$ (2.25), $\text{P}_{\text{bas}}\text{--Se} = 2.264$ (2.23), $\text{P}_{\text{bas}}\text{--P}_{\text{bas}} = 2.270$ (2.24).

porting Information (S.I.). Relative energy values within isomer pairs and essential data on geometries are presented in Table 2.

For both pairs of isomers the calculations yielded the species with the cage bound through the base as being

slightly more stable than the “apical” isomer, with increasing energy separation between the isomers on going from the models of the P_4S_3 derivative to those of P_4Se_3 . Although this trend qualitatively agrees with the NMR spectroscopic data, it is difficult to rationalize in terms of a restricted number of factors, due to the complexity of the systems and to the fine balance in energies. However, the following considerations may shed some light on the preferences for the two coordination modes of these cage molecules with respect to the $\text{Ru}(\eta^5\text{-C}_5\text{Me}_5)(\text{dppe})$ metal–ligand system.

From calculations at the consistent B3LYP/6–31G(d) level on the isolated P_4S_3 and P_4Se_3 molecules, the (twofold degenerate) HOMO for both systems has important contributions from the P_{bas} atoms. An MO with dominant P_{apc} contribution lies $69.0 \text{ kJ}\cdot\text{mol}^{-1}$ (P_4S_3) and $89.9 \text{ kJ}\cdot\text{mol}^{-1}$ (P_4Se_3) below the HOMO; the situation is not substantially altered if calculations on the cages are performed at a better level, such as the B3LYP/6–31++G(2d). This suggests that, based only on these energy differences, a P_{bas} atom should be a better donor than P_{apc} , particularly for the P_4Se_3 cage, towards empty metal orbitals. Conversely, according to the localized orbital picture of the NBO approach, the lone pair (lp) of a P_{bas} atom lies at lower energy than the P_{apc} lp; however, the gap between the two decreases (from 66.9 to $26.3 \text{ kJ}\cdot\text{mol}^{-1}$) on going from P_4S_3 to P_4Se_3 .

The NBO analysis generally describes, at second-order perturbation theory level, the interaction between the cage and the metal as mostly consisting of donation from the P_{bas} (or P_{apc}) lp into a lobe of an antibonding orbital of the metal–ligand moiety. The **5bas** model, however, is peculiar since (a) the P_{bas} lp is involved in more than one fractional interaction of the above type, (b) Ru empty orbitals, rather than Ru-based antibonding acceptor MOs, are involved in

such interactions and (c) no significant repulsive interactions of the P_{bas} lp with bonding (filled) orbitals of the metal moiety are detected, contrary to the other three models. These features, pointing to a comparatively higher strength of the $P_{\text{bas}}-\text{Ru}$ interaction in the **5bas** system, result from several small changes in MO compositions and energies, and are difficult to analyse in deeper detail. Overall, the cage molecules transfer electron density to the metal moiety, with apparently negligible back-donation, according to the NBO perturbation treatment (but see below: changes in antibonding orbital populations). The amount of transferred charge (q , a.u.) increases from apical to basal coordination and, for a given coordination mode, increases on going from P_4S_3 to P_4Se_3 . The, perhaps slightly overestimated, $|q|$ are: 0.196 **10apc**, 0.214 **10bas**, 0.199 **5apc** and 0.228 **5bas**.

The cage molecules undergo only small changes in geometry upon coordination, although some trends are evident. The most significant of these may be rationalized by considering the variations in the populations of the bonding and (to a greater extent) antibonding localized orbitals, according to the NBO picture. In particular, the 0.02 Å (P_4S_3) or 0.04 Å (P_4Se_3) elongation of the $P_{\text{apc}}-\text{S/Se}$ bonds upon coordination in the apical mode (Table 2, including footnote c for the free cage molecules) can be accounted for by the modest decrease (1%) in the $P_{\text{apc}}-\text{S/Se}$ bonding populations and considerable increase in the antibonding ones (e.g., from 0.137 to an average 0.205 a.u. for **10apc**) for both cages. Similarly, for basal coordination by P_4S_3 (**10bas**; trends are strictly similar for the Se analog **5bas**) where the $P(2)-S(1)$ bond elongates by 0.012 Å and the $S(1)-P(1)$ bond shortens by 0.021 Å with respect to the computed free cage values, the corresponding antibonding orbital NBO populations increase (from 0.080 to 0.153 a.u.) and, respectively, decrease (from 0.137 to 0.103 a.u.). Such trends, predominantly indicative of back donation, may be reconciled with the overall flow of negative charge towards the metal moiety considering that complex charge redistributions are allowed by the topology of the cage molecules.

As noted for the P_4S_3 molecule in a related study,^[11] calculated bond lengths for both cage molecules here, whether coordinated or uncoordinated (Table 2), are slightly larger than the experimental values;^[10,21–23] this could be due in part to effects of thermal motion causing an apparent shortening of the bonds in the diffraction experiments on the free cage molecules. The calculated Ru-P(dppe) distances (Table 2) are longer than generally found for dppe ruthenium complexes with a similar environment, although the experimental values span a large range, e.g., from 2.28^[24] to 2.41 Å.^[25] Also, the calculated Ru-C are longer than the experimental ranges for $\eta^5\text{-C}_5\text{Me}_5$ (2.20–2.26 Å,^[26] 2.25–2.34 Å^[25]). These results may reflect the limitations of the present approach (nature of the particular DFT potential^[27–29] and of the metal ECP^[20] used), but may be caused by overcrowding around the metal atom in the present systems. A theoretical study on the adducts of the present cage molecules with BX_3 ($X = \text{Br}, \text{I}$) and NbCl_5 Lewis acids^[12] has reached quite similar conclusions for the

energetics, although more detailed comparisons are prevented by differences between the systems.

Conclusions

$[\text{Ru}(\eta^5\text{-C}_5\text{Me}_5)(\text{L-L})]^+$ metal fragments are rather specific for basal coordination by the P_4X_3 cage molecules, independently of moderate changes in the L–L ligand. Combined with previous results for $[(\text{triphos})\text{Re}(\text{CO})_2\text{-(P}_4\text{X}_3)]\text{CF}_3\text{SO}_3$ compounds,^[11] the present ones suggest that the coordination mode of the P_4X_3 molecules through one of the basal phosphorus atoms is competitive with the apical mode and the balance between the two coordination isomers may be set by subtle properties of the metal fragments and by minor features of their interactions with the cage molecules.

Experimental Section

All reactions and manipulations were performed under an atmosphere of dry oxygen-free argon. THF was freshly distilled from sodium; dichloromethane, *n*-hexane, methanol and ethanol were degassed and flushed with argon prior to use. The ^1H , $^{31}\text{P}\{^1\text{H}\}$ and $^{13}\text{C}\{^1\text{H}\}$ NMR spectra were measured on a Varian Gemini g300bb spectrometer, equipped with a variable-temperature unit, operating at 300 MHz (^1H), 121.46 MHz (^{31}P) and 75.46 MHz (^{13}C). Chemical shifts are relative to tetramethylsilane and to H_3PO_4 85% as external standards at $\delta = 0.00$ ppm; coupling constants are given in Hertz. Analytical data for carbon, hydrogen and sulfur were obtained from the Microanalytical Laboratory of the Department of Chemistry of the University of Firenze. The ligands 1,2-bis(diphenylphosphanyl)ethane (Aldrich), dppe, bis(diphenylphosphanyl)methane (Aldrich), dppm, *cis*-1,2-bis(diphenylphosphanyl)ethylene (Aldrich), dppe, and (1-diphenylarsanyl-2-diphenylphosphanyl)ethane (Pressure Chemical Company), dpadppe, were used as purchased. P_4S_3 was purchased from Fluka AG. and recrystallized from toluene before use. P_4Se_3 was synthesized from red phosphorus and grey selenium as described previously.^[30] The complexes $[\text{Ru}(\eta^5\text{-C}_5\text{Me}_5)\text{Cl}(\text{L-L})]$ [$\text{L-L} = \text{dppe}$ (**1**) and dppm (**2**)] were synthesized according to the literature method.^[14] The complexes $[\text{Ru}(\eta^5\text{-C}_5\text{Me}_5)\text{Cl}(\text{L-L})]$ [$\text{L-L} = \text{dppe}$ (**3**) and dpadppe (**4**)] are new and were synthesized by the same procedure reported for **1** and **2**.^[14] The ^1H , and $^{13}\text{C}\{^1\text{H}\}$ NMR spectroscopic data of the compounds, together with the $^{31}\text{P}\{^1\text{H}\}$ NMR data of the phosphane ligands are reported here. For the minor isomers of **10–13** the weak ^1H resonances of the L–L ligand aliphatic protons and the ^{13}C signals were not observed. The uninformative ^1H and $^{13}\text{C}\{^1\text{H}\}$ signals of phenyl groups of the L–L ligands and of the tetraphenylborate anion, occurring in the expected regions of 6.8–7.5 and 133.5–130.0 ppm, respectively, are not reported.

Syntheses

[Ru($\eta^5\text{-C}_5\text{Me}_5$)Cl(dppe)] (3**):** Yellowish orange microcrystals, yield 85%. $\text{C}_{36}\text{H}_{37}\text{ClP}_2\text{Ru}$ (668.2): calcd. C 64.7, H 5.6; found C 64.5, H 5.8. ^1H NMR (CDCl_3 , 298 K): $\delta = 2.01$ [s, 15 H, br, $\text{C}_5(\text{CH}_3)_5$] and 7.85 (s, 2 H, br, *PCH*). $^{13}\text{C}\{^1\text{H}\}$ NMR (CDCl_3 , 298 K): $\delta = 6.2$ [br. s, $\text{C}_5(\text{CH}_3)_5$], 94.5 [br. s, $\text{C}_5(\text{CH}_3)_5$] and 137.5 (br. s, *PCH*). $^{31}\text{P}\{^1\text{H}\}$ NMR (CDCl_3 , 298 K): $\delta = 94.5$ (s).

[Ru($\eta^5\text{-C}_5\text{Me}_5$)Cl(dpdppe)] (4**):** Yellowish orange microcrystals, yield 82%. $\text{C}_{36}\text{H}_{39}\text{AsClPRu}$ (714.1): calcd. C 60.6, H 5.5; found C

60.4, H 5.6. ¹H NMR (C₆D₆, 298 K): δ = 1.67 [s, 15 H, br, C₅(CH₃)₅], 2.40 (s, 2 H, br, AsCH₂) and 2.76 (s, 2 H, br, PCH₂). ¹³C{¹H} NMR (C₆D₆, 298 K): δ = 10.1 [br. s, C₅(CH₃)₅], 24.1 (br. s, AsCH₂), 28.7 (br. s, PCH₂) and 87.6 [br. s, C₅(CH₃)₅]. ³¹P{¹H} NMR (C₆D₆, 298 K): δ = 76.4 (s).

[Ru(η^5 -C₅Me₅)(dppe)(P₄Se₃)]BPh₄ (5): P₄Se₃ (175 mg, 0.5 mmol) dissolved in THF (30 mL) at 40 °C was added to a THF solution (15 mL) of **(1)** (335 mg, 0.5 mmol); neat NaBPh₄ (250 mg, 0.7 mmol) was then added. The resulting solution was stirred at room temperature for 2 h. An ethanol/light petroleum (1:1) solution (15 mL) was then slowly added, and orange microcrystals were obtained by slowly evaporating the resulting solution. Yield 60%. C₆₀H₅₉BP₆RuSe₃ (1314.7): calcd. C 54.8, H 4.5; found C 54.5, H 4.7. ¹H NMR (CD₂Cl₂, 298 K): δ = 1.56 [dt, 15 H, ⁴J(H-P_Q) = 3.0, ⁴J(H-P_A) = 1.8 Hz, C₅(CH₃)₅], 2.38, 2.82 (m, 4 H, PCH₂). ¹³C{¹H} NMR (CD₂Cl₂, 298 K): δ = 10.8 [s, C₅(CH₃)₅], 27.3 [t, ¹J(C-P_A) = 22.6 Hz, PCH₂], 98.5 [s, C₅(CH₃)₅]. ³¹P{¹H} NMR (CD₂Cl₂, 298 K): δ = 72.2 [2 P, d, ²J(P_A-P_Q) = 27.5 Hz].

The compounds [Ru(η^5 -C₅Me₅)(L-L)(P₄Se₃)]BPh₄ [L-L = dpmm (6), dppt (7) and dpadppe (8)] were prepared by the same procedure as for **5**.

[Ru(η^5 -C₅Me₅)(dpmm)(P₄Se₃)]BPh₄ (6): Yield 62%. C₅₉H₅₇BP₆RuSe₃ (1300.7): calcd. C 54.5, H 4.4; found C 54.8, H 4.3. ¹H NMR [(CD₃)₂CO, 298 K]: δ = 1.79 [dt, 15 H, ⁴J(H-P_Q) = 3.0, ⁴J(H-P_A) = 2.1 Hz, C₅(CH₃)₅], 3.91, 4.72 (1 H each, m, PCH₂). ¹³C{¹H} NMR (CD₂Cl₂, 298 K): δ = 11.7 [s, C₅(CH₃)₅], 46.1 [t, ¹J(C-P_A) = 24.0 Hz, PCH₂], 98.6 [s, C₅(CH₃)₅]. ³¹P{¹H} NMR (CD₂Cl₂, 298 K): δ = 2.4 [2P, d, ²J(P_A-P_Q) = 29.7 Hz].

[Ru(η^5 -C₅Me₅)(dppt)(P₄Se₃)]BPh₄ (7): Yield 60%. C₆₀H₅₇BP₆RuSe₃ (1312.7): calcd. C 58.9, H 4.4; found C 58.6, H 4.4. ¹H NMR (CD₂Cl₂, 298 K): δ = 1.59 [dt, 15 H, ⁴J(H-P_Q) = 2.7, ⁴J(H-P_A) = 1.8 Hz, C₅(CH₃)₅]; the ¹H and ¹³C signals of the ligand CH group were masked by the aromatic resonances. ¹³C{¹H} NMR [(CD₃)₂CO, 298 K]: δ = 11.6 [s, C₅(CH₃)₅], 98.6 [s, C₅(CH₃)₅], 130.9 [vt, ¹J(C-P_A) = 5.8 Hz, PCH₂]. ³¹P{¹H} NMR [(CD₃)₂CO, 298 K]: δ = 76.7 [2P, d, ²J(P_A-P_Q) = 31.9 Hz].

[Ru(η^5 -C₅Me₅)(dpadppe)(P₄Se₃)]BPh₄ (8): Yield 63%. C₆₀H₅₉AsBP₅RuSe₃ (1358.7): calcd. C 53.0, H 4.4; found C 53.1, H 4.3. ¹H NMR [(CD₃)₂CO, 298 K]: δ = 1.66 [dd, 15 H, ⁴J(H-P_Q) = 2.7, ⁴J(H-P_A) = 1.8 Hz, C₅(CH₃)₅], 2.38 (s, 2 H, br, AsCH₂), 2.78 (s, 2 H, br, PCH₂). ³¹P{¹H} NMR [(CD₃)₂CO, 298 K]: δ = 74.4 [1P, dd, ²J(P_A-P_Q)], 33.5 [³J(P_A-P_M) = 6.0 Hz].

[{Ru(η^5 -C₅Me₅)(dppe)}₂(P₄Se₃)](BPh₄)₂ (9): [Ru(η^5 -C₅Me₅)Cl(dppe)] (**1**) (170 mg, 0.25 mmol) dissolved in THF (15 mL) was added to **5** (263 mg, 0.20 mmol) in THF (20 mL). The resulting solution was stirred at room temperature for 1 h; neat NaBPh₄ (96 mg, 0.28 mmol) was then added. Orange microcrystals were subsequently obtained by adding an ethanol/light petroleum (1:1) mixture (15 mL) and by concentrating the solution. Yield 50%. C₁₂₀H₁₁₈B₂P₈Ru₂Se₃ (2268.7): calcd. C 63.5, H 5.2; found C 63.3, H 5.2. ¹H NMR (CD₂Cl₂, 298 K): δ = 1.48 [30 H, br, C₅(CH₃)₅], 2.43, 2.86 (s, 8 H, br, PCH₂). ¹³C{¹H} NMR (CD₂Cl₂, 298 K): δ = 11.2, 11.5 [s, C₅(CH₃)₅], 28.5, 29.7 [d, ¹J(C-P_A) = 24.0 Hz, (PCH₂)], 99.1, 101.1 [s, C₅(CH₃)₅]. ³¹P{¹H} NMR (CD₂Cl₂, 298 K): δ = 71.1 [2P, d, P_A, ²J(P_A-P_Q) = 30.4 Hz], 72.0 [2P, d, P_A, ²J(P_A-P_F) = 25.5 Hz].

[Ru(η^5 -C₅Me₅)(dppe)(P₄S₃)]BPh₄ (10): A THF solution (15 mL) of **1** (335 mg, 0.5 mmol) was added to P₄S₃ (110 mg, 0.5 mmol) dissolved in THF (15 mL); neat NaBPh₄ (250 mg, 0.7 mmol) was then

added. The resulting solution was stirred at room temperature for 2 h. An ethanol/light petroleum ether (1:1) solution (15 mL) was then slowly added, and yellow microcrystals were obtained by slowly evaporating the resulting solution. Yield 65%. C₆₀H₅₉BP₆RuS₃ (1174.0): calcd. C 61.4, H 5.1, S 8.2; found C 60.9, H 5.2, S 8.0. Major isomer: ¹H NMR (CD₂Cl₂, 298 K): δ = 1.52 [dt, 15 H, ⁴J(H-P_Q) = 3.3, ⁴J(H-P_A) = 1.5 Hz, C₅(CH₃)₅], 2.40, 2.80 (m, 4 H, PCH₂). ¹³C{¹H} NMR (CD₂Cl₂, 298 K): δ = 10.8 [s, C₅(CH₃)₅], 27.4 [t, ¹J(C-P_A) = 22.4 Hz, PCH₂], 98.6 [s, C₅(CH₃)₅]. ³¹P{¹H} NMR (CD₂Cl₂, 298 K): δ = 69.3 [2 P, d, ²J(P_A-P_Q) = 31.4]. Minor isomer: ¹H NMR (CD₂Cl₂, 298 K): δ = 1.62 [dt, 15 H, ⁴J(H-P_F) = 2.7, ⁴J(H-P_A) = 1.5 Hz, C₅(CH₃)₅]. ³¹P{¹H} NMR (CD₂Cl₂, 298 K): δ = 67.0 [2 P, d, ²J(P_A-P_F) = 28.7 Hz].

The compounds [Ru(η^5 -C₅Me₅)(L-L)(P₄S₃)]BPh₄ [L-L = dpmm (**11**), dppt (**12**) and dpadppe (**13**)] were prepared by the same procedure as for **10**.

[Ru(η^5 -C₅Me₅)(dpmm)(P₄S₃)]BPh₄ (11): Yield 65%. C₅₉H₅₇BP₆RuS₃ (1160.0): calcd. C 61.4, H 5.1; found C 60.9, H 5.2. Major isomer: ¹H NMR (CD₂Cl₂, 298 K): δ = 1.76 [dt, 15 H, ⁴J(H-P_Q) = 3.3, ⁴J(H-P_A) = 2.1 Hz, C₅(CH₃)₅], 3.98, 4.83 (1 H each, m, PCH₂). ¹³C{¹H} NMR (CD₂Cl₂, 298 K): δ = 10.6 [s, C₅(CH₃)₅], 45.4 [t, ¹J(C-P_A) = 26.1 Hz, PCH₂], 97.9 [s, C₅(CH₃)₅]. ³¹P{¹H} NMR (CD₂Cl₂, 298 K): δ = 1.9 [2 P, d, ²J(P_A-P_Q) = 30.8 Hz]. Minor isomer: ¹H NMR (CD₂Cl₂, 298 K): δ = 1.70 [s, 15 H, br, C₅(CH₃)₅]. ³¹P{¹H} NMR (CD₂Cl₂, 298 K): δ = 1.31 [2 P, d, ²J(P_A-P_F) = 31.1 Hz].

[Ru(η^5 -C₅Me₅)(dppt)(P₄S₃)]BPh₄ (12): Yield 68%. C₆₀H₅₇BP₆RuS₃ (1172.0): calcd. C 61.5, H 4.9; found C 61.2, H 4.9. Major isomer: ¹H NMR (CD₂Cl₂, 298 K): δ = 1.56 [dt, 15 H, ⁴J(H-P_Q) = 3.0, ⁴J(H-P_A) = 1.8 Hz, C₅(CH₃)₅]; the CH vinyl proton of the ligand was masked by the aromatic resonances. ¹³C{¹H} NMR (CD₂Cl₂, 298 K): δ = 10.7 [s, C₅(CH₃)₅], 98.8 [s, C₅(CH₃)₅], 129.0 [vt, ¹J(C-P_A) = 5.4 Hz, PCH₂]. ³¹P{¹H} NMR (CD₂Cl₂, 298 K): δ = 75.7 [2 P, d, ²J(P_A-P_Q) = 32.5 Hz]. Minor isomer: ¹H NMR (CD₂Cl₂, 298 K): δ = 1.70 [s, 15 H, br, C₅(CH₃)₅]. ³¹P{¹H} NMR (CD₂Cl₂, 298 K): δ = 73.2 [2 P, d, ²J(P_A-P_F) = 31.6].

[Ru(η^5 -C₅Me₅)(dpadppe)(P₄S₃)]BPh₄ (13): Yield 70%. C₆₀H₅₉AsBP₅RuS₃ (1218.0): calcd. C 59.2, H 4.9; found C 59.1, H 4.8. Major isomer: ¹H NMR (CD₂Cl₂, 298 K): δ = 1.58 [dd, 15 H, ⁴J(H-P_Q) = 3.3, ⁴J(H-P_A) = 1.8 Hz, C₅(CH₃)₅], 2.44 (s, 2 H, br, AsCH₂), 2.78 (s, 2 H, br, PCH₂). ¹³C{¹H} NMR (CD₂Cl₂, 298 K): δ = 10.8 [s, C₅(CH₃)₅], 20.9 [d, ²J(C-P_A) = 11.0 Hz, AsCH₂], 30.1 [dd, ¹J(C-P) = 32.7, ³J(C-P_Q) = 5.4 Hz, PCH₂], 97.3 [s, C₅(CH₃)₅]. ³¹P{¹H} NMR (CD₂Cl₂, 298 K): δ = 73.1 [1 P, dd, ²J(P_A-P_Q) = 36.0, ³J(P_A-P_M) = 7.0]. Minor isomer: ¹H NMR (CD₂Cl₂, 298 K): δ = 1.58 [dd, 15 H, ⁴J(H-P_Q) = 3.3, ⁴J(H-P_A) = 1.8 Hz, C₅(CH₃)₅]. ³¹P{¹H} NMR (CD₂Cl₂, 298 K): δ = 76.1 [1 P, d, ²J(P_A-P_F) = 27.4 Hz].

Computational Procedures

Calculations were performed on models of the [Ru(η^5 -C₅Me₅)(dppe)(P₄S₃)]⁺ and [Ru(η^5 -C₅Me₅)(dppe)(P₄Se₃)]⁺ cations with the GAUSSIAN 98 suite of programs,^[31] using the hybrid HF-DFT B3LYP method.^[27–29] Preliminary geometry optimizations (not reported), were performed (a) on simplified models of the P₄S₃ derivative, where the methyl and phenyl groups were replaced by hydrogen atoms, using the 6–31G(d,p) basis set^[32] for the non-metal atoms and the LANL2DZ valence functions and effective core potential (ECP)^[20] for ruthenium and (b) on “complete” models, with no simplifying replacements of methyl and phenyl groups using, however, the lower quality 3–21G (C, H) and

3–21G* (P, S)^[33,34] basis sets for the non-metal atoms. In these preliminary calculations coordination by the P₄S₃ cage molecule through the apical phosphorus atom, and through one of its basal P atoms, was considered, no symmetry was imposed. Overall, these calculations revealed a delicate energy balance between geometrical isomers differing in the mode of coordination by the cage. Moreover, for each mode the calculations on the “complete” models revealed the existence of several energy minima, characterized by small differences in the corresponding geometries. This was probably due to the effects of numerous non-bonded interactions between the bulky groups surrounding the metal atom. Computationally demanding geometry optimizations on the “complete” models at the better B3LYP/6–31G(d) level (with LANL2DZ Ru functions as above) were then performed, starting from the lowest-energy arrangement detected in the preliminary search for each of the P₄S₃ coordination modes of the [Ru(η⁵-C₅Me₅)(dppe)(P₄S₃)]⁺ system. The two corresponding models for the [Ru(η⁵-C₅Me₅)(dppe)(P₄Se₃)]⁺ cation were obtained by substitution of Se for S in the former P₄S₃ optimized models and underwent optimization in turn. Frequency calculations were performed for the four final models [a small negative (imaginary) frequency of –11 cm^{–1} for the system with apically bound P₄Se₃, at the verge of significance for residual rotational motion of CH₃ groups, was confidently ignored] and unscaled zero-point energy corrections were applied. The interpretation of results was aided by natural bond orbital (NBO) analyses.^[35,36] For graphics MOLDEN^[37] and ORTEP^[38,39] were employed.

Acknowledgments

We acknowledge financial support from the Italian Ministero dell'Istruzione, dell'Università e della Ricerca. Thanks are also expressed to INTAS for supporting this research (project 00-00018).

- [1] J. G. Riess, in *Rings, Cluster and Polymers* (Ed. A. H. Cowley), ACS Symp. Ser., **1983**, vol. 232, p. 17.
- [2] M. Di Vaira, P. Stoppioni, M. Peruzzini, *Comments, Inorg. Chem.* **1990**, *11*, 1–19.
- [3] M. Di Vaira, P. Stoppioni, *Coord. Chem. Rev.* **1992**, *120*, 259–279.
- [4] J. Wachter, *Angew. Chem. Int. Ed.* **1998**, *37*, 751–768.
- [5] L. Y. Goh, *Coord. Chem. Rev.* **1999**, *185–186*, 257–276.
- [6] L. Y. Goh, W. Chen, R. C. S. Wong, *Organometallics* **1999**, *18*, 306–314.
- [7] A. W. Cordes, R. D. Joyner, R. D. Shores, E. D. Dill, *Inorg. Chem.* **1974**, *13*, 132–134.
- [8] R. Jefferson, H. F. Klein, J. F. Nixon, *J. Chem. Soc., Chem. Commun.* **1969**, 536–537.
- [9] M. Di Vaira, M. Peruzzini, P. Stoppioni, *Inorg. Chem.* **1983**, *22*, 2196–2198.
- [10] M. Di Vaira, M. Peruzzini, P. Stoppioni, *J. Organomet. Chem.* **1983**, *258*, 373–381.
- [11] E. Guidoboni, I. de Rios, A. Ienco, L. Marvelli, C. Mealli, A. Romerosa, R. Rossi, M. Peruzzini, *Inorg. Chem.* **2002**, *41*, 659–668.
- [12] C. Aubauer, E. Irran, T. M. Klapoetke, W. Schnick, A. Schulz, J. Senker, *Inorg. Chem.* **2001**, *40*, 4956–4965.
- [13] A. Adolf, M. Gonsior, I. Krossing, *J. Am. Chem. Soc.* **2002**, *124*, 7111–7116.
- [14] I. de los Rios, M. J. Tenorio, J. Padilla, M. C. Puerta, P. Valerga, *J. Chem. Soc., Dalton Trans.* **1996**, 377–381.
- [15] R. J. Haines, A. L. Du Preez, *J. Organomet. Chem.* **1975**, *84*, 357–367.
- [16] P. M. Treichel, D. A. Komar, P. J. Vincenti, *Inorg. Chim. Acta* **1984**, *88*, 151–152.
- [17] I. de los Rios, J.-R. Hamon, P. Hamon, C. Lapinte, L. Toupel, A. Romerosa, M. Peruzzini, *Angew. Chem. Int. Ed.* **2001**, *40*, 3910–3912.
- [18] C. A. Ghilardi, S. Midollini, A. Orlandini, *Angew. Chem. Int. Ed. Engl.* **1983**, *22*, 790–791.
- [19] M. Di Vaira, M. Peruzzini, P. Stoppioni, *J. Chem. Soc., Dalton Trans.* **1985**, 291–295.
- [20] P. J. Hay, W. R. Wadt, *J. Chem. Phys.* **1985**, *82*, 270–283.
- [21] Y.-C. Leung, J. Waser, S. van Houten, A. Vos, G. A. Wiegiers, E. H. Wiebenga, *Acta Crystallogr.* **1957**, *10*, 574–582.
- [22] E. Keulen, A. Vos, *Acta Crystallogr.* **1959**, *12*, 323–329.
- [23] J. R. Rollo, G. R. Burns, W. T. Robinson, R. J. H. Clark, H. M. Dawes, M. B. Hursthouse, *Inorg. Chem.* **1990**, *29*, 2889–2894.
- [24] M. El-Khateeb, B. Wolfsberger, W. A. Schenk, *J. Organomet. Chem.* **2000**, *612*, 14–17.
- [25] K. Mauthner, K. Mereiter, R. Schmid, K. Kirchner, *Organometallics* **1994**, *13*, 5054–5061.
- [26] F. Morandini, A. Dondana, I. Munari, G. Pilloni, G. Consiglio, A. Sironi, M. Moret, *Inorg. Chim. Acta* **1998**, *282*, 163–172.
- [27] A. D. Becke, *J. Chem. Phys.* **1993**, *98*, 5648–5652.
- [28] A. D. Becke, *J. Chem. Phys.* **1993**, *98*, 1372–1377.
- [29] C. Lee, W. Yang, R. G. Parr, *Physical Review B: Condensed Matter and Materials Physics* **1988**, *37*, 785–789.
- [30] P. Stoppioni, M. Peruzzini, *Gazz. Chim. Ital.* **1988**, *118*, 581–582.
- [31] M. J. Frisch, G. W. Trucks, H. B. Schlegel, G. E. Scuseria, M. A. Robb, J. R. Cheeseman, V. G. Zakrzewski, J. A. Montgomery, Jr., R. E. Stratmann, J. C. Burant, S. Dapprich, J. M. Millam, A. D. Daniels, K. N. Kudin, M. C. Strain, O. Farkas, J. Tomasi, V. Barone, M. Cossi, R. Cammi, B. Mennucci, C. Pomelli, C. Adamo, S. Clifford, J. Ochterski, G. A. Petersson, P. Y. Ayala, Q. Cui, K. Morokuma, D. K. Malick, A. D. Rabuck, K. Raghavachari, J. B. Foresman, J. J. V. Cioslowski, A. G. Ortiz, B. B. Baboul, G. Stefanov, G. Liu, A. Liashenko, P. Piskorz, I. Komaromi, R. Gomperts, R. L. Martin, D. J. Fox, T. Keith, M. A. Al-Laham, C. Y. Peng, A. Nanayakkara, C. Gonzalez, M. Challacombe, P. M. W. Gill, B. Johnson, W. Chen, M. W. Wong, J. L. Andres, C. Gonzalez, M. Head-Gordon, E. S. Replogle, J. A. Pople, *Gaussian 98, Revision A. 7*, Gaussian, Inc., Pittsburgh PA, **1998**.
- [32] R. Ditchfield, W. J. Hehre, J. A. Pople, *J. Chem. Phys.* **1971**, *54*, 724–728.
- [33] J. S. Binkley, J. A. Pople, W. J. Hehre, *J. Am. Chem. Soc.* **1980**, *102*, 939–947.
- [34] W. J. Pietro, M. M. Francl, W. J. Hehre, D. J. DeFrees, J. A. Pople, J. S. Binkley, *J. Am. Chem. Soc.* **1982**, *104*, 5039–5048.
- [35] E. D. Glendening, A. E. Reed, J. A. Carpenter, F. Weinhold, *NBO Version 3.1*.
- [36] J. P. Foster, F. Weinhold, *J. Am. Chem. Soc.* **1980**, *102*, 7211–7218.
- [37] G. Schaftenaar, J. H. Noordik, *J. Comput.-Aided Mol. Design* **2000**, *14*, 123–134.
- [38] C. K. Johnson, *ORTEP*, Report ORNL-5138, Oak Ridge National Laboratory, Oak Ridge/TN, USA, **1976**.
- [39] L. J. Farrugia, *J. Appl. Crystallogr.* **1997**, *30*, 565.

Received July 17, 2003

Early View Article

Published Online November 19, 2003